Scientific paper

Oxygen Barrier and Thermomechanical Properties of Poly (3-hydroxybutyrate-co-3-hydroxyvalerate) Biocomposites Reinforced with Calcium Carbonate Particles

Semra Kirboga* and Mualla Öner*

Chemical Engineering Department, Yildiz Technical University, 34210, Istanbul, Turkey

** Corresponding author: E-mail: skirboga@yildiz.edu.tr and muallaoner@gmail.com*

Received: 05-31-2019

Abstract

This study aimed to prepare poly (3-hydroxybutyrate-co-3-hydroxyvalerate), biocomposites with incorporating various percentages of calcium carbonate using extrusion processing. Calcium carbonate was synthesized in the absence and presence of poly(vinyl sulfonic acid). The polymorph and morphology of calcium carbonate chanced with the introduction of poly(vinyl sulfonic acid). The rhombohedral calcite was obtained in the absence of poly(vinyl sulfonic acid). Rhombohedral calcite transformed into spherical vaterite with the addition of poly(vinyl sulfonic acid). The influence of filler contents on the properties of poly (3-hydroxybutyrate-co-3-hydroxyvalerate) composites was studied. The structure and properties of poly (3-hydroxybutyrate-co-3-hydroxyvalerate)/ calcium carbonate biocomposites were investigated by XRD, FTIR, TGA, DSC, SEM, OTR and DMA. The nucleation effect of the calcium carbonate on the crystallization of poly (3-hydroxybutyrate-co-3-hydroxyvalerate) was observed in the DSC and XRD measurements by increasing crystallinity of poly (3-hydroxybutyrate-co-3-hydroxyvalerate). It was shown that the variation of the barrier properties of biocomposites was influenced by polymorph and morphology of calcium carbonate. The addition of 0.5 wt% of the rhombohedral calcite and spherical vaterite increased the barrier properties by 25% and 12%, respectively compared to neat polymer. The dynamic mechanical properties of composites based on rhombohedral calcite and spherical vaterite in poly (3-hydroxybutyrate-co-3-hydroxyvalerate) matrix were investigated. The storage modulus increases by adding both particles in the composites over a wide range of temperature (-30 to 150 °C) where the reinforcing effect of calcite and vaterite was confirmed. At the same loading level, rhombohedral calcite led to more increase in the storage modulus, while less increase in storage modulus was observed in the presence of spherical vaterite particles.

Keywords: Poly (3-hydroxybutyrate-co-3-hydroxyvalerate); biocomposite; calcite; vaterite; barrier properties; thermal properties

1. Introduction

Over the past centuries, plastics have been used increasingly because they have many good properties over other materials. The vast majority of plastics are mostly products from the petroleum. They deplete petrochemical feedstock and remain for thousands of years in the environment. Plastics have been accumulating leading to massive waste, which contributes to pollution problems in our ecosystem.[1,2] All of these burdens have led to tremendous efforts to research and development of environmentally friendly polymers. Many biodegradable materials have been developed as alternatives to conventional nondegradable polymers.[3] The Poly(hydroxyalkanoates) (PHAs) are biodegradable polymers produced through the fermentation of sugars, lipids, alkanes, alkenes and alkanoic acids using numerous Gram-positive and Gram-negative bacteria. They can be used in various applications such as biomedical industry, packaging, coatings, films, electronics, sensors, foams, and energy applications because of their remarkable physical properties and biodegradability.[1,3] Poly (3-hydroxybutyrate, PHB) which is the well-studied polymer is the member of PHAs family. Its application is limited by the poor processability and high brittleness of polymer. The copolymer of PHB like poly (3-hydroxybutyrate-co-3-hydroxyvalerate) (PHBV) was developed to

improve the ductility and processability of the polymer. The mechanical properties of PHBV are better than PHB.[2] The increase in the composition of HV causes a decrease in the melting point of composites. The presence of polyhydroxyvalerate (PHV) in PHB matrix increases the processability of the polymer. The content of 3-HV in PHBV is effective on the mechanical properties of PHBV composites. However, PHBV has limitations like high crystallinity and a small processing window, which need to be overcome before converting it into useful products. Concerning these shortcomings, fillers can be used in the preparation of poly (3-hydroxybutyrate-co-3-hydroxyvalerate) composites for reducing its production price and enhancing properties.[2,3]

Composites made from biopolymers and inorganic nanoparticles will find significant potential in many applications due to their enhanced properties and processing characteristics. Braga et al. studied the effect of titanium dioxide particles on properties of PHBV.[1] It was observed that the addition of titanium dioxide in the PHBV matrix decreases the glass transition temperature of the material. PHB/TiO_2 nanocomposites were prepared and characterized by using different techniques. TGA results showed that PHB composites containing TiO_2 particles presented an increment in thermal stability. TiO_2 particles act as a nucleating agent for PHB[1]. Öner et al.[3,4] studied the effect of h-BN as the potentially interesting material on the enhancement of properties of PHBV. The resulting PHBV nanocomposites showed an increase in oxygen permeability, thermal stability and crystallinity.[3,4] The effect of adding an electrospun PHBV/CuO coating over compression molded PHBV films on the different properties of nanocomposites were investigated. CuO addition using electrospinning enhanced the nanoparticles dispersion but did not significantly modify the oxygen permeability, mechanical or optical properties.[5]

Thermomechanical behavior of fiber reinforced PHBV was investigated by Adam et al.[6] The DMA results showed that fibers cause an increase in storage modulus and loss modulus.[6] Biodegradable nanocomposites were prepared using nanofibrillated cellulose (NFC) as the reinforcement and PHBV as the polymer matrix. DMA results showed that the modulus for 10 wt% NFC reinforced nanocomposite increased 28% compared to neat PHBV at 25 °C, while the storage modulus increased 137% at 100 °C.[7] Residual lignocellulosic flour was used as a natural filler in PHBV-based composites. A significant increase of rubbery modulus was observed by DMA. The result was ascribed to reinforcing effect of the filler and/or the increase of the degree of crystallinity.[8] The hybrid composites from wood fiber, talc and PHBV were developed by using extrusion-injection molding. The elastic modulus of the polymer increased by 75% wt. talc loading with the supplementary increase of 120% at additional 20 wt% wood fiber loading below the glass transition temperature. The increase was by 103% and 208%, respectively above the Tg. It was suggested that talc and wood fiber in PHBV were posing a restriction to the free rotation of the molecular chains above Tg.[9] The effects of incorporating hyperbranched polymers (HBPs) and different nanoclays on the mechanical properties of PHBV were investigated. Poly(maleic anhydride-alt-1-octadecene) (PA) was used as a crosslinking agent. The storage modulus of PHBV decreased with the addition of 12% (HBP+PA) in the glassy region of the polymer. This result was attributed to the free volume enhancement of the PHBV chains.[10] PHBV/bamboo pulp fiber (BPF) composites were prepared by melt compounding and injection molding. The storage modulus of the composites was found to increase across the whole temperature range from glassy to rubbery states.[11] The composites were developed by incorporating agro-residues into PHBV by melt mixing technique. The tensile and storage modulus of PHBV was improved by a maximum of 256% and 308% with the reinforcement of 30 wt% agricultural byproducts.[12] PHBV was reinforced with cellulose nanowhiskers (CNW) using the solvent casting method. DMA results showed that storage modulus of the PHBV increased with the addition of CNW at temperatures higher than the PHBV glass transition temperature.[13] PHBV and glycerol-plasticized cornstarch blends were prepared by melt extrusion in the presence of an organoclay. The significant increase in the dynamic storage modulus was observed, reaching 251% at 25 C and 275% at 50 C.[14] PHBV/husk flour (OHF) were prepared by melt compounding. The surface treatment of OHF by trimethoxyoctadecylsilane (TMOS) was performed by thermo-chemical vapor deposition. The storage modulus of PHBV increase by 36% after adding 20 wt. % of untreated OHF. The effect of silane treatment of filler on PHBV/OHF composites leads to an increase in storage modulus compared to the untreated one.[15] Fabrication of PHBV/natural bamboo fiber was carried out by injection molding. The storage modulus of composites improved by 157% and 173% at 30 and 40 wt% fiber content at 25 °C, respectively.[16] PHBV/multiwalled carbon nanotubes (MWNT) were prepared by melt blending. DMA results showed that CNT's did not affect the Tg but increased storage modulus with an increase in MWNT content.[17]

In this study, PHBV composites containing calcite and vaterite particles with different sizes, morphology, and specific surface areas were processed and characterized to elucidate the effects of particles on composite properties. Calcium carbonate ($CaCO_3$) used in composites was synthesized in the absence and presence of the polymeric additive. Calcium carbonate ($CaCO_3$) is highly abundant mineral in the earth's crust and is used in many industries such as pigment, cosmetic, plastic, rubber, paper, and electronics.[18] $CaCO_3$ used in the plastic industry leads to a decrease in surface energy, opacity and surface gloss.[19] The impact strength, elongation at break and stiffness of polymer can be increased with using calcium carbonate with the suitable particle size.[19] $CaCO_3$ exhibits three polymorphic forms; vaterite, aragonite, and calcite, listed in order of increasing stability.[18] While calcite is the most thermo-

dynamically stable form of calcium carbonate, vaterite and aragonite are thermodynamically unstable forms of calcium carbonate. Unstable forms of calcium carbonate can be stabilized with using additives. Vaterite can be used in biomedical and industrial fields due to its higher solubility and its higher dispersion.[20] Calcite used in the plastic industry leads to a decrease in surface energy, opacity and surface gloss. Moreover, the impact strength, elongation at break and stiffness can be increased with using calcite having the suitable particle size.[19]

Organic and inorganic fillers have been used in polymeric materials for many years to modify properties, reduce material costs and improving the processing. It is known that understanding the effect of the shape, volume fraction, size and dispersion of particles on the composite's properties is really important.[21,22] We report here our continuing research effort to design biocomposite with desirable properties by reinforcing calcium carbonate particles with a twin screw extruder. Polymer composites containing particles of two different morphology, rhombohedral calcite and spherical vaterite were prepared through melt processing route with different concentrations to elucidate the role of the particle morphology, on the different properties of the resulting composites. Although the incorporation of calcium carbonate particles into polymers such as polypropylene [19,23–25] have been carried out, to the best of our knowledge, no information is available on the incorporation of calcite and vaterite particles in PHBV. The study conducted on the effect of spherical and rhombohedral particle shape showed that rhombohedral calcite led to more increase in the storage modulus and oxygen barrier properties, while less increase in storage modulus and barrier properties were observed in the presence of spherical vaterite particles at the same loading level.

2. Experimental Section

2. 1. Materials

PHBV, the biopolymer with 8 mol% hydroxyvalerate (HV) content was supplied by ADmajoris Company, France under the trade name MAJ'ECO FN000HA in a pelletized form suitable for melt extrusion. Calcium chloride ($CaCl_2$) and sodium carbonate (Na_2CO_3) (reagent grade) were from Merck. Poly(vinyl sulfonic acid) (PVS) of 5000 MW was from Aldrich.

2. 2. Preparation of Calcium Carbonate ($CaCO_3$) Particles

The experiments were conducted in a 0.5 dm^3 water-jacketed reactor providing a constant-temperature at 25 ± 3 °C. 100 mM of calcium and 100 mM of carbonate solutions were used to synthesize calcium carbonate. Calcium carbonate was precipitated by mixing equal volumes (100 cm^3) of $CaCl_2$ and Na_2CO_3 solutions. First, calcium solution was added to the reactor. Sodium carbonate solution and polymer solution were quickly poured into the reactor. The complete experimental procedures were reported previously.[18,20] The schematic representation of the synthesis of calcium carbonate was given in Figure 1. Ultrasound was applied for 5 minute by use of an ultrasound probe into the reaction. The crystallization solution was subjected to sonication (Sonics Vibra Cell, 20 kHz and 13 mm with threaded end and replaceable tip probe) at room temperature. The amplitude value was 50% whereas polymer concentration was 0.25 g/L. Precipitated crystals were washed with distilled water. The obtained $CaCO_3$ particles were filtered through a 0.2 μm cellulose nitrate membrane filter, dried at 100 °C for 24 h.

2. 3. Preparation of PHBV/$CaCO_3$ Composites

PHVB/$CaCO_3$ composites were prepared by the melt mixing method. Although there are many different methods to produce composites, melt processing is generally useful due to more economical, more flexible for the formulation. Moreover this process involves compounding and fabrication facilities commonly used in commercial practice.[3] A twin-screw extruder (Rondol Microlab, England) with L/D ratio 20 was used for preparing com-

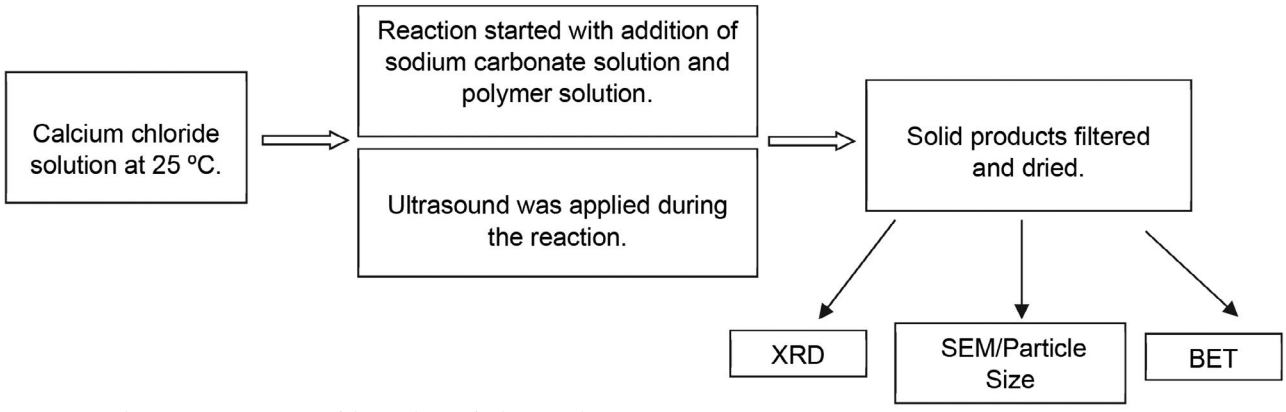

Figure 1. Schematic representation of the synthesis of calcium carbonate.

Table 1. Experimental conditions for obtaining the composites

Sample Code	Particles	Amount of Particles (wt. %)	Sample Code	Particles	Amount of Particles (wt. %)
Neat PHBV	–	–			
PHBV/C0.1	Calcite	0.1	PHBV/V0.1	Vaterite	0.1
PHBV/C0.5	Calcite	0.5	PHBV/V0.5	Vaterite	0.5
PHBV/C1.0	Calcite	1.0	PHBV/V1.0	Vaterite	1.0
PHBV/C3.0	Calcite	3.0	PHBV/V3.0	Vaterite	3.0

posites. The percentages of $CaCO_3$ used in PHVB/ $CaCO_3$ composites were 0.1, 0.5, 1 and 3 wt%. The screw speed was 80 rpm, and the operating temperatures of the five extruder zones (from feed to die) were set to 90–135–160–160–155 °C. The extrudate was cooled in air and pelletized for further use. Sheet samples were prepared using a hot-cold press machine (Gülnar Makine, Turkey).[3] The sheet thickness of the prepared samples was around 0.8 mm. The experimental conditions were given in Table 1 with the sample names carrying the information of synthesis conditions. C (calcite) shows calcium carbonate obtained in the absence of PVS, V (vaterite) indicates calcium carbonate obtained in the presence of PVS. The capital letter shows the species of calcium carbonate used in the composites. The number in the code of composite indicates species amount in the composites (wt. %). For instance, while PHBV/C0.1 denotes composite synthesized in the presence of 0.1 wt. % of calcium carbonate obtained in the absence of PVS, PHBV/V0.1 shows composite synthesized in the presence of 0.1 wt. % of calcium carbonate obtained in the presence of PVS.

2. 4. Characterization of Particles and Composites

X-ray diffraction analysis of the particles and composite samples were carried out using a PanalyticalX'pert Pro PW 3040/60 powder diffractometer operating with Cu Kα radiation in operating at 40 mA and 45 kV. The 2θ range was from 5° to 90° at a scan rate of 0.026° step^{-1}. The samples crystal morphology was analyzed by scanning electron microscopy (FEI-Philips, XL 30 ESEM-FEG). PHBV nanocomposite sheet samples were analyzed by scanning electron microscopy (FEI-Philips, XL 30 ES-EM-FEG) to evaluate the dispersion of the nanoparticles inside the PHBV matrix. Particle sizes of the particles were investigated using XRD (Scherrer equation), laser diffraction and SEM. We investigated the particle-size distribution of the powders by Laser particle sizer Fritsch Analysette 22-Compact. The Brunauer, Emmett and Teller method was used to investigate the surface area of crystals. Nitrogen sorption isotherms according to the multiple-point BET (Brunauer, Emmett and Teller- COSTECH Kelvin Sorptometer 1042) method was used to determine the specific surface area (SSA) of the $CaCO_3$ crystals. Calcium carbonate samples were first outgassed at 80 °C. The nitrogen adsorption isotherm has been performed by additions of gaseous nitrogen to the tube containing the sample at 77 K.[18] FTIR analysis was performed by using BRUKER Alpha-P in the 400–4000 cm^{-1} region at a resolution 4 cm^{-1}. FT-IR analysis was given in ATR-reflectance mode.

2. 5. Dynamic Mechanical Analysis of Samples

Dynamic mechanical analysis (DMA) was carried out with Perkin Elmer DMA8000 (dynamic mechanical analyzer). Film extension mode in the temperature range of –30 °C to 150 °C at a heating rate of 2 °C min^{-1} was applied in order to investigate the dynamic properties of samples in single cantilever mode at 1 Hz. The dimensions of the test samples were 10.40 mm × 10 mm. Storage modulus E', loss modulus E", and tan δ = E"/E' were determined and recorded versus temperature during the tests.

2. 6. Thermal Properties of PHBV Composites

Thermo Gravimetric Analyzer (Perkin Elmer Pyris Diamond DTA–TG was used to characterize the thermal stability of the films. About 10 mg of each film sample was taken in a standard aluminum cup and heated in the temperature ranged from 25 to 800 °C with heating rate of 10 °C/min under a nitrogen flow of 40 mL/min. DSC measurements were performed on Perkin Elmer Diamond DSC. The polymer composites were analyzed in three steps with a heating and cooling rate of 10 °C/min. To determine the thermal properties of the polymer composites, samples of 5 mg mass in an aluminum crucible under 50 mL/min nitrogen atmosphere was used. In the first heating step, samples were heated from 0 °C to 200 °C. In order to erase thermal history of the material, the samples were kept at this temperature for 2 min. In the second step (cooling run), the samples were subsequently cooled to 0 °C at a rate of 10 °C/min. Similarly, the samples were kept at 0 °C for 2 min. In the third step, polymer composites were re-heated from 0 °C to 200 °C. The thermal parameters like melting and the crystallization temperatures (Tm and Tc), the melting and the crystallization enthalpies (ΔH_m and ΔH_c) were obtained from DSC analysis. The following formula was used to calculate the crystallinity of polymer composites:[4]

$$\chi_C(\%) = \left[\frac{\Delta H_m}{\left(W_{PHBV} \times \Delta H_m^{ref}\right)}\right] \times 100 \quad (1)$$

Where ΔH_m shows melting enthalpy of sample, ΔH_m^{ref} is theoretical melting enthalpy for 100% crystallized PHBV (146 J/g^{-1})[26] and W_{PHBV} is weight fraction of PHBV in the composite.

2. 7. Barrier Properties of PHBV Composites

Systech Illinois instruments Model 8001 oxygen permeation analyzer was used to measure oxygen transmission rates (OTR) of neat PHBV and PHBV composites films. Polymer composites were analyzed according to continuous-flow cell method approved by ASTM D3985–05. The tests were conducted at 23 °C, 0% relative humidity and 1 atm pressure with highly purified oxygen (99.99%) and nitrogen (99.99%) gases.[4] Analysis was terminated when OTR graphics reached the steady condition. The permeability (OP) was calculated by multiplying the measured steady state transmission rate by the average sample thickness. At least two separate films were measured for each sample.

3. Result and Discussion

3. 1. Characterization of the Particles

X-ray diffraction pattern of calcium carbonate crystals obtained in the absence of additive and the presence of PVS was given in Figure 2. In the absence of PVS, peaks were observed at scattering angles (2θ) of 29.4° for reflection (104), at 35.9° for reflection (110) and 39.5° for reflection (113).[18] XRD analysis exhibits the characteristic reflections for calcite with scanning angle 23.04, 29.47, 36.05, 39.48, 43.19, 47.54, 48.53, 57.3, 60,61, 64.60 and h k l (012), (104), (110), (113), (202), (018), (116), (122), (214) and (300) respectively.[18] The diffraction peaks of the crystals can be indexed as the (104) reflection of pure calcite. All intensity peaks of XRD patterns of $CaCO_3$ synthesized in the absence of PVS matched the $CaCO_3$ described in standards. The main characteristic peaks of vaterite were observed in $CaCO_3$ sample obtained in the presence of PVS (Figure 2). Vaterite peaks appear at scattering angles (2θ) of 24.92° for reflection (110), at 26.99° for reflection (112) and 32.78°for reflection (114). While a weak peak at 29.26° belongs to calcite was observed, semiquantitative analysis of the XRD results using the Rietveld method with HighScore Plus software showed that the percentage of vaterite was 97%.

It is known that the crystallization mechanism of biominerals can change due to polar functional groups such as $-CO_2H$, $-PO_3H$, $-SO_3H$.[27,28] Even if the functional groups are present in low concentrations, they have enormous effects on the growth, nucleation, morphology, and polymorphism of the crystals. The required first step of interaction between functional groups and the crystallizing species is the adsorption of the functional groups onto the pre-nuclear cluster.[18,20] In this work, the observed changes of the precipitate morphology in the presence of PVS indicate that polymer affects the nucleation and crystal growth calcium carbonate. We can suggest that incorporation of PVS into the crystallization medium slows down the nucleation growth rate of calcium carbonate and therefore calcite growth is poisoned. As the calcite growth is inhibited due to polymer poisoning, formation of vaterite was promoted and PVS stabilized the particles in solution as the vaterite polymorph.

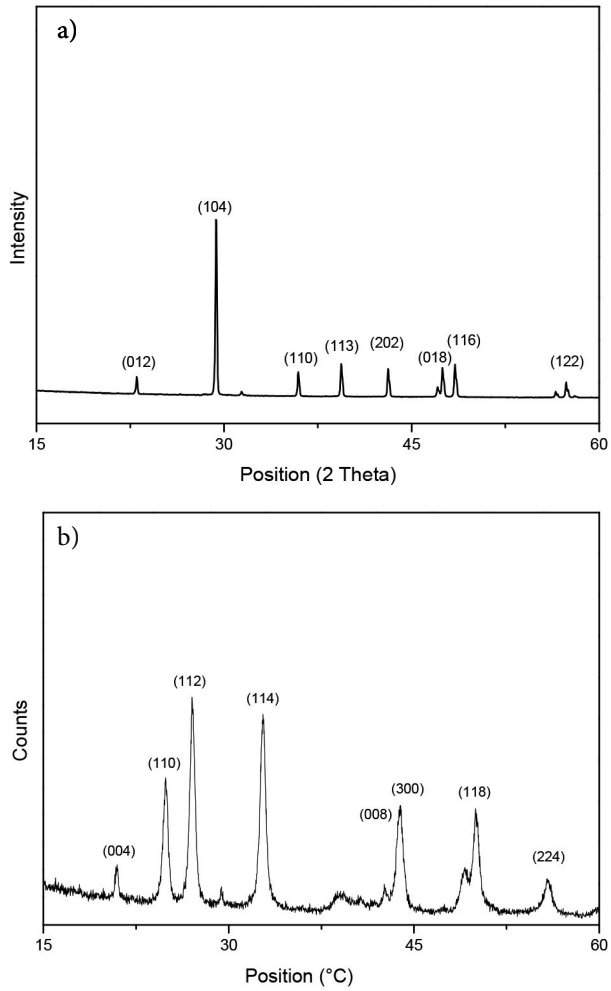

Figure 2. X-ray diffraction patterns of $CaCO_3$ obtained in the (a) absence and (b) presence of PVS.

SEM analysis also confirmed the morphological changes. Figure 3 shows the morphology of calcium carbonate crystals obtained from SEM investigation. The typical rhombohedral form of calcite was observed in the absence of polymer (Figure 3a). The common shape of calcite is a rhombohedron which consists of (104) faces. It is known both by experiment and by simulation, that the

(104) is the most stable surface of calcite. It is also the most common morphology of the natural calcium carbonate samples.[29]

The particle size of calcium carbonate was analyzed from SEM micrographs. The dimensions of the minimum of 50 crystals in each sample were measured from SEM photomicrographs. The mean crystal size of rhombohedral calcite was 3.6 x 3.3 ± 0.75 μm. When the particles were produced in the presence of PVS, a significant change in the morphology of calcium carbonate was obtained as evidenced by SEM pictures. PVS lead to the formation of spherical vaterite (Figure 3b). The results of SEM analysis are coherent with the XRD results. The mean crystal size of spherical vaterite was 1.52 ± 0.47 μm. The change in the morphology of calcium carbonate could result from the strong interaction of PVS and calcium carbonate. The nucleation and crystal growth of the calcite and vaterite was affected by the introduction of PVS.[27] Meng et al. explained morphological changes by the adsorption of sulfonic groups on calcium carbonate.[30] The interactions between PVS and crystals may result in the phase transformation of calcite to vaterite.

The analysis of particle size and the size distribution of calcium carbonate was carried out with using Fritsch Analysette 22 Compact. The median crystal sizes of were 5.38 ± 2.22 μm and 1.62 ± 0.66 μm for calcium carbonate obtained in the absence of PVS and in the presence of PVS, respectively. A narrow particle size distribution was obtained with the introduction of PVS. The specific surface areas were measured as 0.34 m^2/g and 12.08 m^2/g for calcium carbonate obtained in the absence of PVS and in the presence of PVS, respectively.

3. 2. SEM Pictures of the Composites

Calcite and vaterite particles were used to produce composites at different particle loadings. The dispersion of the particles achieved in PHBV matrix was observed using SEM for the PHBV/C and PHBV/V composites. Figure 4 shows the cross section SEM images of the surfaces of composites containing 1.0% of PHBV/C and PHBV/V. As shown in Figure 4 for 1.0 wt. % calcium carbonate, the calcite (Figure 4a) and vaterite (Figure 4b) appeared uniformly dispersed and distributed to the individual level in the PHBV

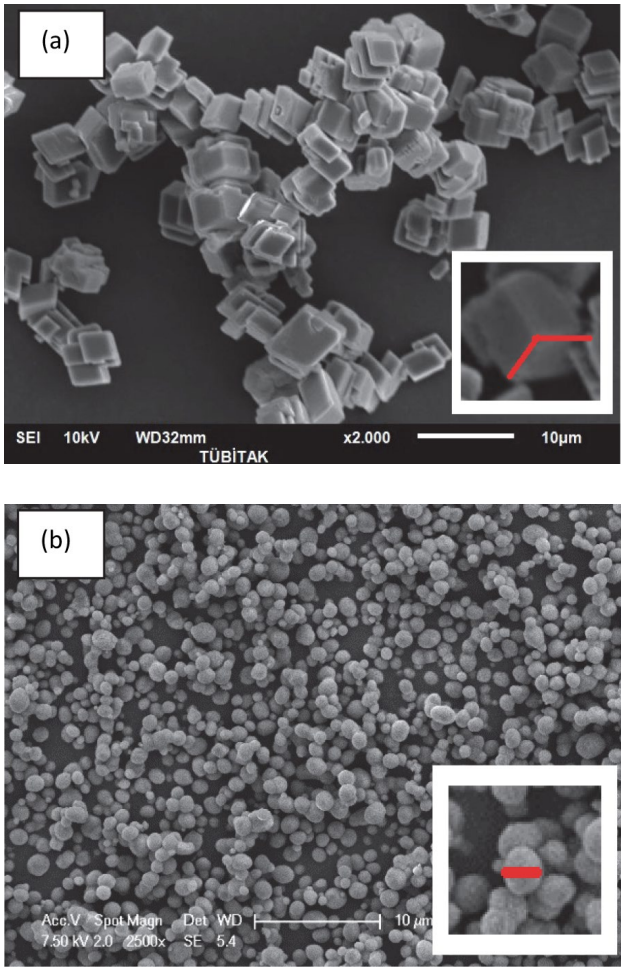

Figure 3. SEM photographs of $CaCO_3$ obtained in the (a) absence of additive and (b) presence of PVS.

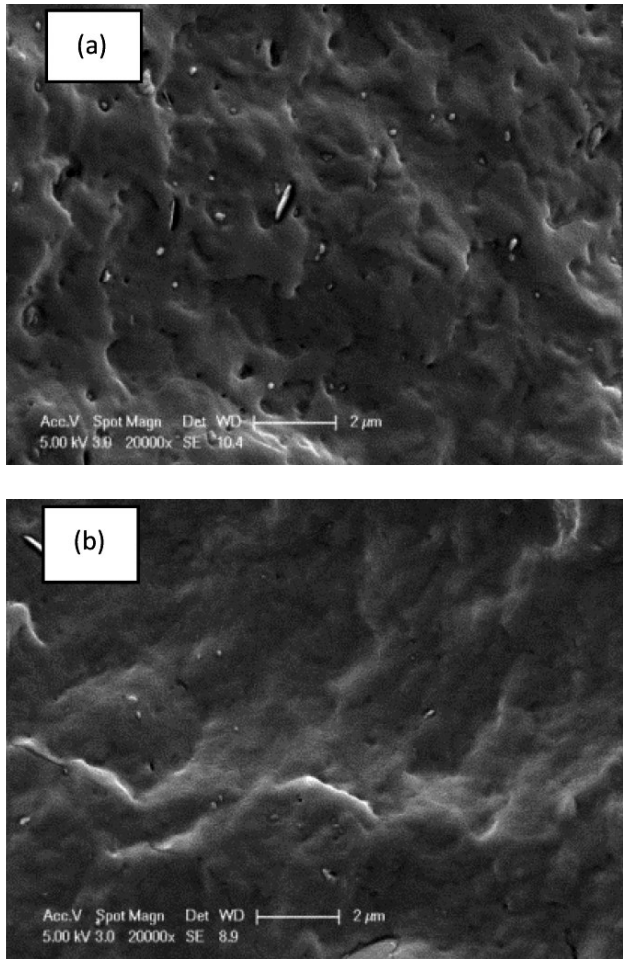

Figure 4. SEM photographs of composites obtained in the presence of (a) 1.0% of calcite and (b) 1.0% of vaterite.

matrix. The edges of individual particles are visible at the fracture surface, and no particle aggregates were observed.

3. 3. XRD and FTIR Analysis of the Composites

XRD analysis is commonly used for the interpretation of composite structure. Figure 5 shows the XRD patterns of biocomposites. The XRD patterns of PHBV exhibited characteristic 2θ peaks at 13.6°(020), 17.1°(110), 19.9°(021), 21.7°(101), 22.3°(111), 25.5°(121), 27.1°(040), 30.3°(002).[3] As shown in Figure 5, all composites show the reflections at the same values for the neat PHBV. It is clear that the unit cell of biopolymer does not change with the addition of calcium carbonate. There is no effect of calcium carbonate on the crystallization of PHBV. The composite can be crystallized in its typical crystalline form. When the intensity of (020) reflection of neat PHBV was compared, the intensity of (020) reflection increased with the addition of calcium carbonate (Figure 5).

XRD of PHBV and $CaCO_3$ exhibit major peaks around 13–32° scan angle interval. So, in this region, it is an evident that characteristic peak of neat PHBV can be overlap with characteristic peak of $CaCO_3$. However, in the case of composite samples, the intensity of the characteristic diffraction peak located at 2θ of at 55° appear to increase compared to neat PHBV (Figure 6). This result shows the inclusion of the $CaCO_3$ particles within polymeric matrix.

The peak broadening of XRD reflection can be used to estimate the crystallite size in a direction perpendicular to the crystallographic plane based on the Scherrer's formula as follows:

$$L = \frac{k\lambda}{BCos\theta} \quad (2)$$

where L is the mean crystallite size in nm, k is the shape factor, B is the broadening of the diffraction line measured at half of its maximum intensity. B was determined by full width at half maximum (FWHM) for the diffraction peak under consideration. The shape factor k becomes 0.9 when FWHM is used for B. λ is the wavelength of monochromatic X-ray beam and θ is the Bragg diffraction angle.[2] Both the size of the crystallites responsible for the Bragg

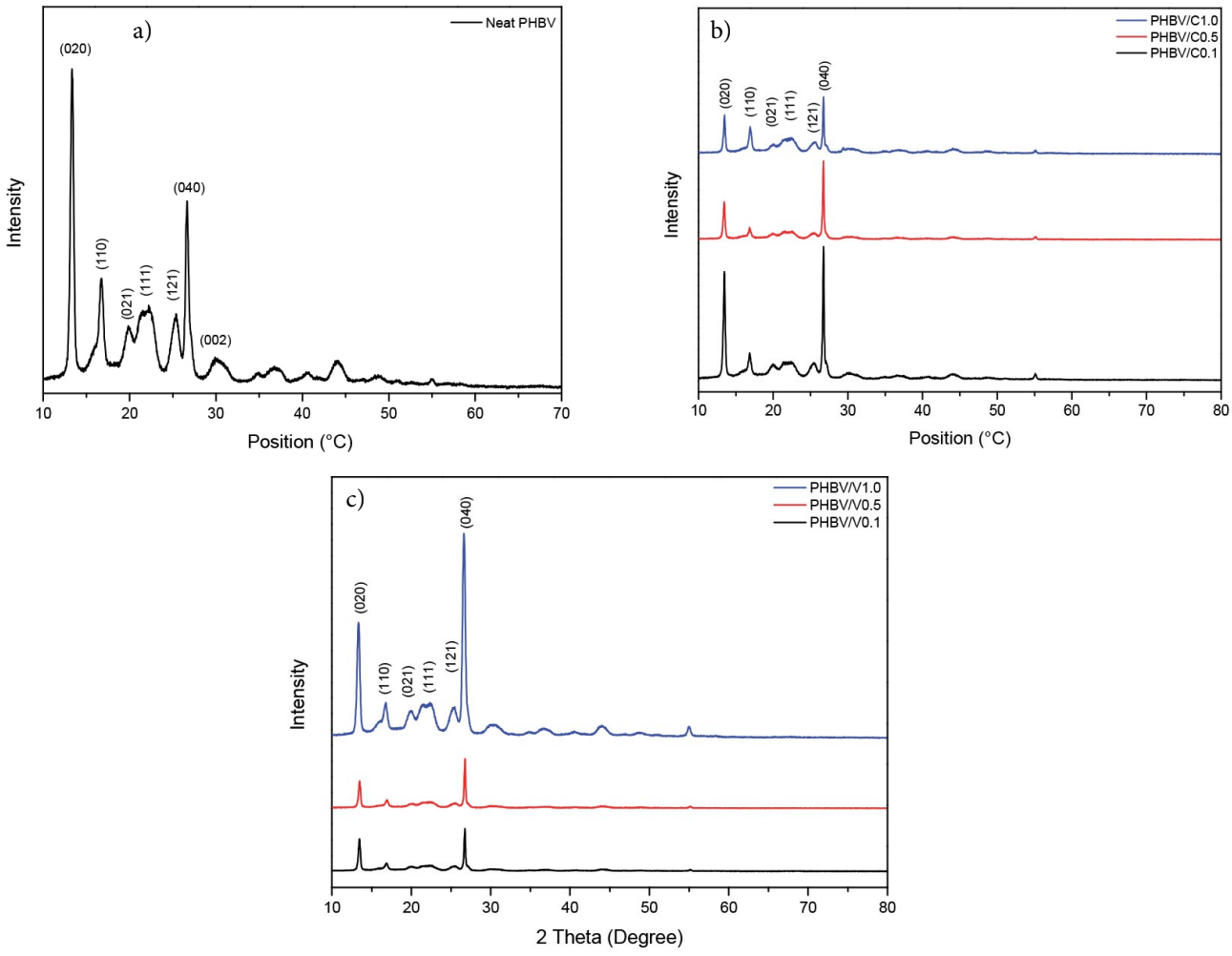

Figure 5. The X-ray diffraction pattern of (a) Neat PHBV, (b) PHBV/C composites and (c) PHBV/V composites.

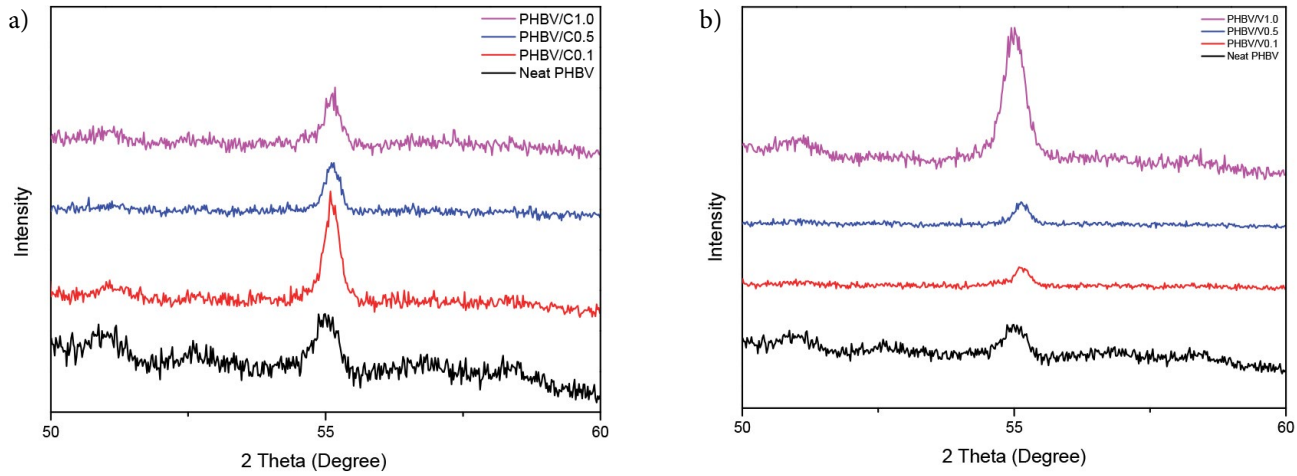

Figure 6. The X-ray diffraction pattern of (a) PHBV/C composites and (b) PHBV/V composites at 2θ of at 55°.

reflection (020) and the ratio of (020)/(110) and (020)/(021) were given in Table 2.

The crystallite size L [nm] calculated for the (020) reflection peak using Scherrer's equation is in the range of 27.10–45.17 nm for composites as opposed to 20.32 nm for neat PHBV. This increase in the crystallite size of (020) crystal plane in the composites with addition of particles shows that nanoparticles provoke the increase in the degree of crystallinity. For this purpose, Crystallinity index (*CI*) values from XRD measurement were calculated for composites samples based on the (020) peak of PHBV and given in Table 2. The following formula was used for calculating *CI*:[31]

$$CI = \frac{I_{(020)}}{I_{Total}} \times 100 \quad (3)$$

CI results have shown that the $CaCO_3$ addition affects the crystallinity of PHBV. The values are higher for all composite samples. The $CaCO_3$ is a known to behave as a nucleating agent and increases the crystallinity of the polymer matrix.[32]

Table 2. *L* (nm), intensity ratios and *CI* (%) of neat PHBV and its composites from XRD scan

Sample Code	*L* (nm)	(020)/(110)	(020)/(021)	*CI* (%)
Neat PHBV	20.32	1.79	8.56	44.70
PHBV/C0.1	36.95	2.51	12.61	48.43
PHBV/C0.5	33.87	3.57	12.05	55.19
PHBV/C1.0	36.95	4.03	22.78	64.47
PHBV/C3.0	24.69	9.21	15.32	69.73
PHBV/V0.1	27.10	2.46	12.07	48.66
PHBV/V0.5	45.17	3.45	13.06	51.34
PHBV/V1.0	36.95	3.38	14.55	54.55
PHBV/V3.0	27.78	2.77	11.60	57.58

Figure 7 shows the FTIR spectra of neat PHBV and the prepared nanocomposites. PHBV exhibited some characteristic peaks as methyl C–H asymmetric stretching at 3015–2960 cm^{-1}, methylene C–H asymmetric stretching at 2945–2925 cm^{-1}, C=O stretching at 1723–1740

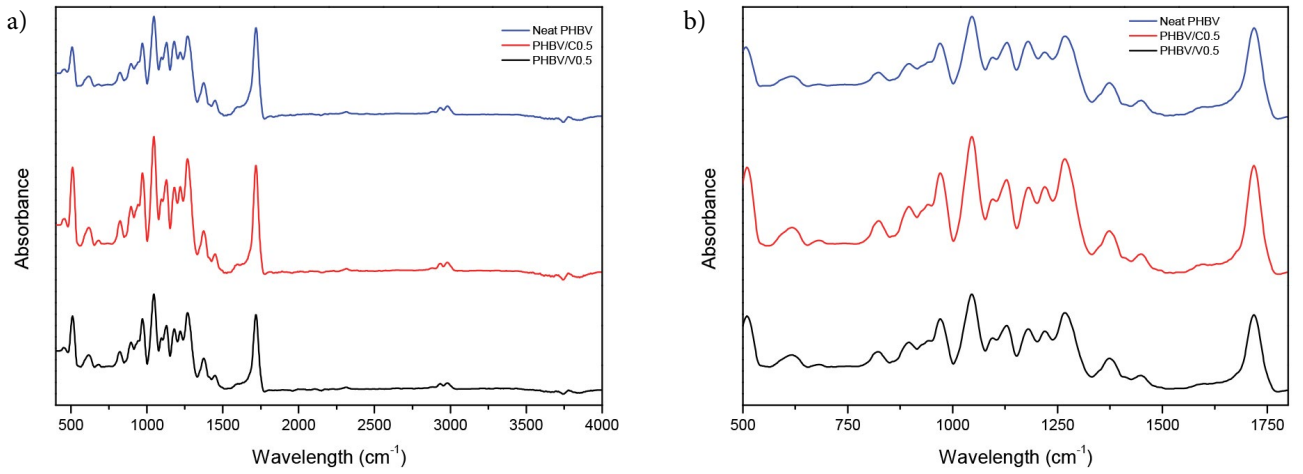

Figure 7. FT-IR spectra of the polymer composites at the (a) 400–4000 cm^{-1} and (b) 500–1800 region.

cm^{-1}, CH_2 wagging at 1320–1159 cm^{-1}, asymmetrical –C–O–C– stretching, symmetrical –C–O–C– stretching at 800–975 cm^{-1}, CH_2 scissoring at 1453–1459 cm^{-1}, C–O stretching at 1065–1030 cm^{-1} and C–C stretching at 979–980 cm^{-1}, respectively.[33] Calcite and vaterite exhibit main characteristic peaks as 712 cm^{-1} and 745 cm^{-1}, respectively.[18] While the peaks at ~1420 and ~874 cm^{-1} indicate the presence of calcite, the peak at ~1070 cm^{-1} shows the presence of vaterite.[18] The peak of calcium carbonate cannot be observed in the spectra of the nanocomposites due to overlapping with the peak of the PHBV. The bands at 1220 to1279 cm^{-1} are crystallinity-sensitive bands for PHBV. The peak intensity in this region is not an absolute measure of the degree of crystallinity but is useful as a comparison criterion.[31] The intensity of the peak in this region increased in the presence of calcium carbonate as can be seen in Figure 7.

3. 4. TGA Analysis of the Composites

Conventional techniques such as extrusion, injection or compression molding can be used to produce PHBV composites.[3] The thermal stability of PHBV is very low so that thermal degradation can take place during the polymer melt processing. Before it was transformed into useful products, the thermal stability of it needs to be developed.[34] Therefore, to investigate the effect of the additive on the thermal decomposition of PHBV is vital for industry and science. The thermogravimetric analysis was used to measure the thermal stability of the PHBV and PHBV/$CaCO_3$ composite. Thermogravimetric analysis was carried out under a nitrogen atmosphere in the temperature range 20–800 °C and the temperature corresponding to initial mass loss (T_i), the temperature of 10% weight loss (T_{10}), the temperature of 50% weight loss (T_{50}) and the temperature of maximum rate of mass loss (T_{max}), were summarized in Table 3. The values of T_i,T_{10},T_{50} and T_{max} of composites slightly increased with the addition of calcium carbonate. When the initial weight loss is taken as a point of comparison, the onset degradation temperature (T_i) for neat PHBV is 264.68 °C. The degradation temperature of composite increased to 274.52 °C and 272.01 °C for PHBV/V0.1 and PHBV/C0.1 composites, respectively.

Table 3. TGA values of PHBV/ $CaCO_3$ composites and neat polymer

Sample Code	T_i (°C)	T_{10} (°C)	T_{50} (°C)	T_{max} (°C)
PHBV	264.68	280.84	292.20	303.66
PHBV/C0.1	272.01	280.56	290.30	308.76
PHBV/C0.5	268.97	280.14	289.42	307.59
PHBV/C1.0	271.68	280.03	289.41	306.28
PHBV/C3.0	273.29	281.49	291.78	304.62
PHBV/V0.1	274.52	280.68	290.40	306.56
PHBV/V0.5	272.10	280.12	288.39	298.97
PHBV/V1.0	268.61	279.48	284.50	292.11
PHBV/V3.0	272.40	278.18	282.88	288.95

3. 5. DSC Analysis of the Composites

DSC analysis was performed to investigate the effect of calcium carbonate on the thermal characteristic of PHBV. The analysis was carried out in 3 steps. Two heating and one cooling cycles were performed for neat polymer and composites. Figure 8 depicts DSC thermograms of first heating (Figure 8a), cooling (Figure 8b), and second heating (Figure 8c) sequences for neat PHBV and PHBV/$CaCO_3$ composites. The results calculated from the DSC heating and cooling curves are summarized in Table 4 for composites with different calcium carbonate contents.

The first melting temperature of the nanocomposite samples shifts to slightly lower temperatures compared to neat PHBV. From Table 4, the heat of melting of the biocomposites are seen to increase with increasing calcium carbonate loading up to 3 wt%. ΔH_{m1} values are in the range of 59–85.4 J/g for composites as opposed to 68.8 J/g for neat PHBV. Crystallization temperature (T_{c1}) and heat of crystallization (ΔH_{c1}) were determined from the DSC cooling runs of these samples. There were no significant changes in the cold crystallization temperatures of the nanocomposite samples compared to neat PHBV. The cold crystallization enthalpy values of the composites vary between 77.8–84.5 J/g, while the enthalpy of the PHBV is 80.5

Table 4. Thermal properties obtained from DSC curves for polymer composites

Sample	First Heating		Cooling		Second Heating		
	T_{m1}(°C)	ΔH_{m1} (J/g)	T_{c1}(°C)	ΔH_c (J/g)	T_{m2}(°C)	ΔH_{m2} (J/g)	χc(%)
Neat PHBV	177.06	68.8	126.63	80.5	175.89	74.6	51.1
PHBV/C0.1	174.87	69.5	124.60	79.9	175.18	78.8	54.0
PHBV/C0.5	173.00	74.7	125.72	80.7	172.98	87.5	60.2
PHBV/C1.0	176.69	72.8	125.88	79.5	176.51	82.6	57.1
PHBV/C3.0	176.05	75.2	125.92	79.6	176.99	81.5	57.5
PHBV/V0.1	175.83	85.4	125.41	84.5	175.29	87.0	59.7
PHBV/V0.5	174.81	76.9	124.93	82.2	174.13	82.9	57.1
PHBV/V1.0	177.63	76.3	126.69	77.8	179.47	79.4	54.9
PHBV/V3.0	178.30	59.0	125.68	78.6	176.29	69.3	48.9

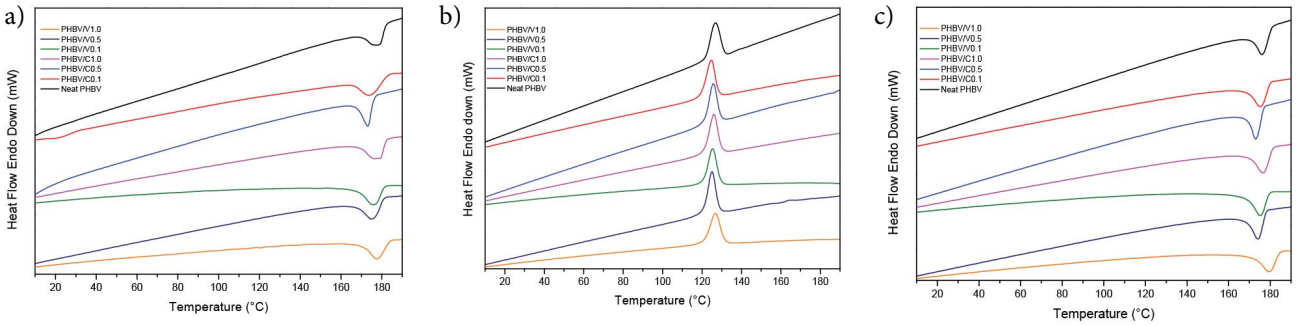

Figure 8. DSC thermograms of polymer composites from the (a) first heating scan, (b) cooling scan, and (c) second heating scan.

J/g. The thermal properties based on the second heating scan of the composites were examined and reported in Table 4. The melting enthalpy and crystallinity of the polymer increased after the incorporation of the calcium carbonate. The values of ΔH_{m2} provide important information about the crystallinity and shows significant variations in the composites. The addition of both calcite and vaterite particles increases the crystallinity of neat PHBV. The addition of calcite increased the degree of crystallinity PHBV from 51.1% to 60.2% at 0.5% wt calcite loading, while addition of vaterite increased from 51.1% to 59.7% at 0.1% wt vaterite loading. This can be explained by the known concept that fillers in a polymer can induce crystal nucleating effects.

3. 6. Oxygen Barrier Properties of the Composites

The oxygen barrier properties of PHBV/$CaCO_3$ composites in different $CaCO_3$ contents were determined by correlating to OTR values of samples with oxygen permeability coefficients. OP is the rate of oxygen transmission through unit area of a flat material of unit thickness induced by unit vapour pressure difference across the material. Relationship between OTR and oxygen permeability were given by the following equation:

$$OP = OTR \times L/\Delta P \quad (4)$$

where OP is the oxygen permeability coefficient (cc mm m^{-2} day^{-1}), OTR is the oxygen transmission rate (cc m^{-2} day^{-1}), L is the film thickness (mm) and ΔP is the difference (bar) between oxygen partial pressure across the film. As shown in Figure 9, the OP of PHBV has a value of 1.35 (cc mm m^{-2} day^{-1}) at 23 °C and the incorporation of calcium carbonate into polymer matrix decreases gas permeability. We can suggest that $CaCO_3$ particles create a barrier for the diffusing gas molecules. OP of PHBV/C0.5 and PHBV/V0.5 shows 25% and 12% improvements, respectively compared to the neat PHBV. When comparing barrier properties between PHBV/calcite and PHBV/vaterite composites, rhombohedral calcite composites showed higher barrier effect than spherical vaterite composites. Maximum decrease in OP value was observed for PHBV/C0.5 composite. OP values do not improve with further increasing the particle content.

The presence of particles changes the crystallinity of crystalline polymers that could affect the permeability. The

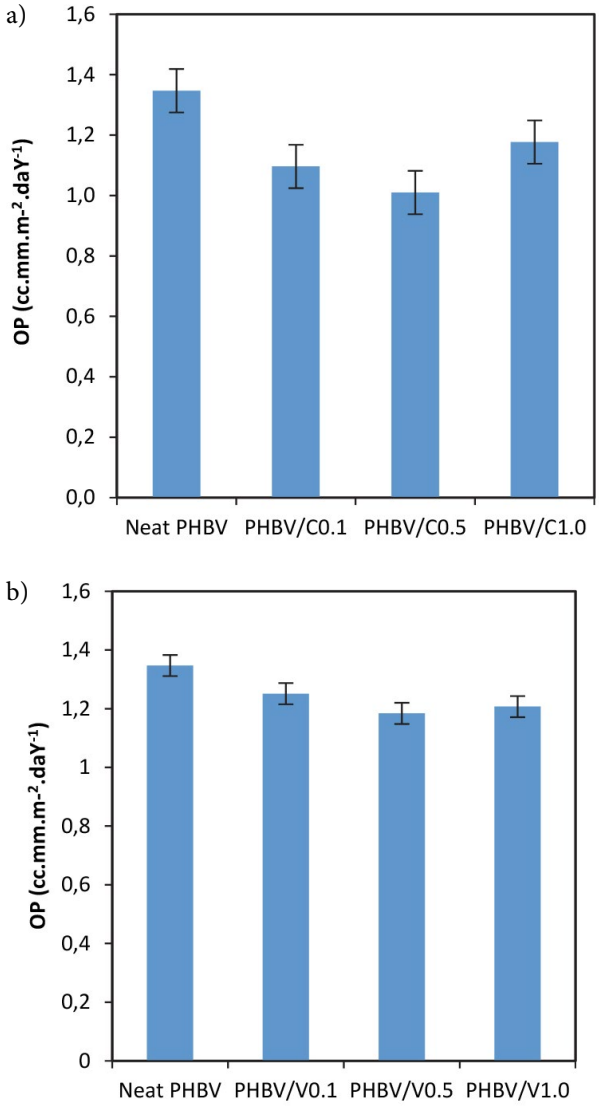

Figure 9. Oxygen permeability (OP) of neat PHBV and PHBV/$CaCO_3$ composites with (a) calcite and (b) vaterite.

percentage of crystallinity values determined from DSC is in the range of 54–60.2 for composites as opposed to 51.1 for neat PHBV. All these findings show that the changes in crystallinity can account for the enhanced barrier properties. It is assumed that gas molecules can diffuse through free volumes at amorphous phase of a semi-crystalline material and no gas diffusion takes place in the crystalline phase.[35] The nanoparticle reduces the free volume for gas diffusion within the polymer, reducing the diffusivity by a tortuous path mechanism. The improvement can be attributed to the increased tortuosity in the presence of $CaCO_3$. A tortuous pathway for the diffusion of gas out of the biocomposite matrix may lead to an increase in barrier properties of biocomposites. This increases the effective path length for diffusion of the gas, thereby reducing the rate of diffusion.

3. 7. Dynamic Mechanical Properties

Dynamic mechanical measurements were performed on neat PHBV and composite samples to investigate the effect of the calcite and vaterite particles on their thermo-mechanical properties. The three parameters were measured: the storage modulus (E'), the loss modulus (E"), and tan delta, the ratio of (E"/E'). The storage modulus (E') and loss modulus (E"), represent the elastic and viscous nature of the polymeric material over a range of temperature.

The storage modulus of PHBV and its composites as a function of the temperature are shown in Figures 10a and 10b, respectively for the calcite and vaterite composites. The storage modulus determines the ability of the polymer to absorb or store energy. In addition, storage modulus is often associated with the stiffness (tensile modulus) of the polymer and is proportional to the energy stored during the loading cycle. It was observed that with the increase in temperature, the storage modulus of neat polymer and its composites gradually decreased. This was due to the softening of the matrix phase in composites. This reduction is expected because of the relaxation of polymer chains as a result of the softening of the matrix phase.

The storage modulus of PHBV in both glassy and rubbery regions is considerably increased after the incorporation of both particles. In Figure 10, it is observed that the storage modulus for nanocomposites is much higher over the whole temperature range compared to neat PHBV. The two particles systems showed different storage modulus values with temperature. Both composites showed reinforcement below and above Tg. The storage modulus enhancement by adding particles can be attributed to the good stress transfer between polymer matrix and particles.

As observed E', the elastic component of the composites increased by 46% and 91% at 0.5 wt.% and 1 wt% calcite loading with respect to neat PHBV respectively, at –10 °C. This enhancement was below the glass transition temperature of PHBV. The increase was by 85% and 139%, respectively above the Tg (140 °C) in the rubbery stage with the same loading trend of calcite in PHBV. The DMA analysis of the vaterite composites show that there is a 74% increase in the storage modulus with 1 wt.% vaterite, as compared to the neat PHBV at –10 °C. The storage modulus increased by 91% for PHBV/V1 composite samples with respect to the neat polymer at 140 °C. When comparing reinforcement between the PHBV/calcite and PHBV/vaterite composites, calcite composites showed higher reinforcement than vaterite composites, both below and above Tg of the polymer matrix. The storage modulus partially declined at 3 wt% content owing to the increased agglomeration of particles. The increase in the storage modulus of PHBV nanocomposites can be attributed to the reducing of the mobility of polymer chains in the presence of particles. All composite samples have higher E' values than neat PHBV as a result of the inherent rigidity of particles. The increase of the storage modulus in the rubbery stage of polymer matrix suggesting that the fillers were posing a restriction to the free rotation of the molecular chains above Tg. The rhombohedral shape of the calcite particles has also played a role in the increment of the

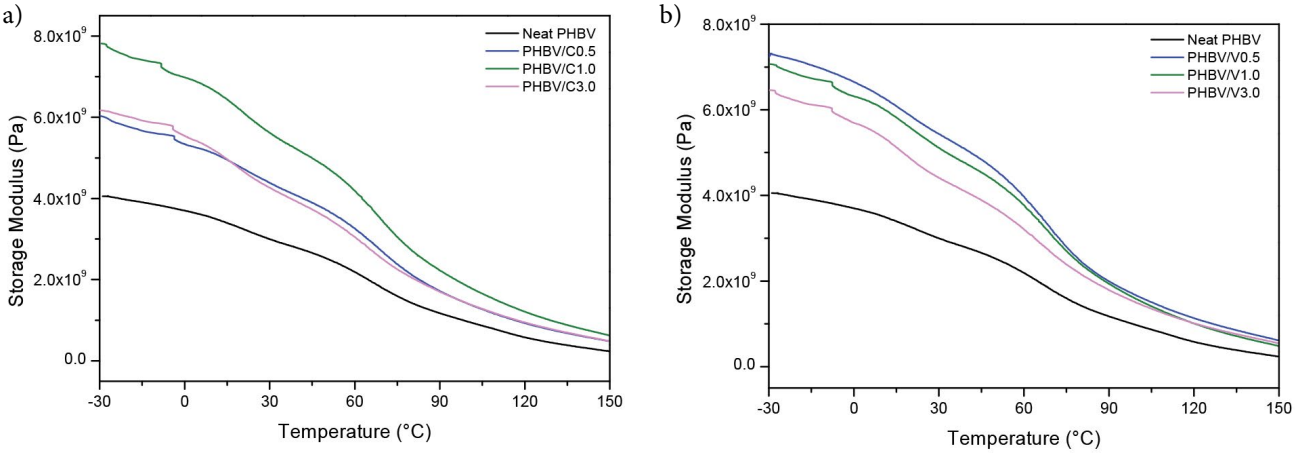

Figure 10. DMA thermographs showing storage modulus for PHBV/$CaCO_3$ composites with (a) calcite and (b) vaterite.

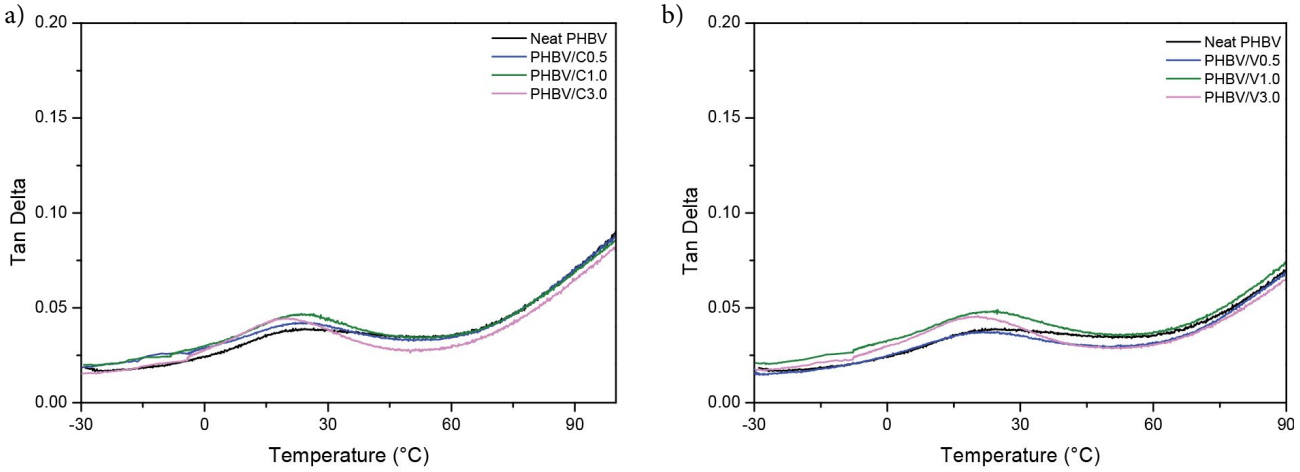

Figure 11. DMA thermographs showing tan delta for PHBV/$CaCO_3$ composites with (a) calcite and (b) vaterite.

modulus when compared to the increase in the spherical shape of vaterite.

Tan delta is the ratio of loss modulus (E") to the storage modulus (E'). It is a measure of the energy dissipated and represents internal friction in viscoelastic material. The glass transition (Tg) could be identified as the peak of the tan delta. Figures 11a and 11b show the tan delta curves of the PHBV and its composites as a function of temperature. The Tg value of the neat PHBV is around 26 °C. It is clear that the tan delta peak for both the composites did not shift significantly as the content of particles increases from 0% to 3%. The tan delta peak temperatures for all of the composites samples fell within 2 °C of the neat PHBV. No significant difference was observed between the Tg of PHBV and composite samples which imply particles did not have any specific effect on the glass transition temperature of the polymer.

The previous studies concerning shape have been shown the relationship between nanocomposite properties and particle shape. The incorporation of particles is to promote the time and heat dependent properties of composites. The particle shape was found to influence the mechanical, barrier and thermal properties of the resulting composites.

The nanoparticles have different polymorphic modifications of calcium carbonate particles namely spherical rhombohedral calcite and elongated ortho-rhombic aragonite were used as reinforcement phases of Nylon6. DMTA analysis showed that calcite nanoparticles increase the glass transition temperature of Nylon 6 up to 12 °C, while a less pronounced increase was recorded for aragonite. It was stated that the most significant effect of calcite particles on the glass transition temperature was due to a large interfacial region.[36]

The effect of filler shape on the nanocomposite reinforcement was investigated by using dynamic-mechanical thermal spectroscopy. Hydroxyapatite (HA) nanofillers with spherical and platelet particle shape were synthesized and used in poly(vinyl acetate, PVAc) matrix. It was observed that the E' decreased with temperature in case of the neat polymer and nanocomposites but the decrease of the E' was stronger for PVAc filled spherical HA filler than for the nanocomposite with platelet HA particles. It was concluded that the higher is the difference between the mobility of the polymer interface and the bulk chains and, the higher is the portion of the interphase chains the higher is the reinforcement.[21]

The epoxy composites, reinforced by boron nitride spheres (s-BN) and flakes (f-BN) were prepared. The effect of filler morphology on thermal conductivity, thermo-mechanical and dielectric properties were investigated. At the same loading level, s-BN with the larger surface area led to a much more significant increase in glass transition temperature and lower storage modulus. The flake BN (f-BN) composites exhibit much higher E' than the spherical BN (s-BN). It was concluded that the high storage modulus of the f-BN composites could be attributed to the particular two-dimensional flake morphology and larger size of the f-BN, which has more significant potential to resist on the deformation of composites at changing temperatures.[37]

4. Conclusions

PHBV composites containing calcium carbonate particles with different morphology and shape were prepared and characterized for understanding the effect of particle characteristics on composite properties. The thermal and barrier properties were investigated by using XRD, FTIR, TG, DSC, OTR and DMA analysis. XRD and DSC studies showed an increase in crystallinity due to the addition of particles. TGA analysis revealed improvement in thermal degradation behaviour of the composites. It was found that the gas barrier properties of composites were improved in the presence of particles within the matrix. The nanoparticle shape has been shown to be a con-

tributing factor to the biocomposite properties. The best barrier properties were obtained for rhombohedral calcite particles. Overall, a 25% improvement in barrier properties was obtained for the PHBV/C0.5 biocomposites in comparison to the neat PHBV sample. According to DSC and XRD results, the composite samples show a high level of crystallinity which explains the lowest oxygen permeability. It is also important to note that the rhombohedral calcite particles may increase more the barriers properties of the polymer by creating a maze or tortuous path that retards the diffusion of gas molecules through the polymer matrix compare to spherical shape vaterite particles. The thermo-mechanical properties of the PHBV composites also improved with the incorporation of the calcium carbonate particles within the polymer matrix. However, rhombohedral calcium carbonate particles exhibited the highest modulus increase compared to neat PHBV. The incorporation of calcite and vaterite particles at 1wt% loading into PHBV matrix enhanced the storage modulus equal to 139% and 91%, respectively at 140 °C. In summary, the properties of the PHBV composites were affected by the particles and the composites with improved mechanical, thermal and barrier properties were obtained.

Acknowledgements

This research has been supported by Research Fund of the Yıldız Technical University. Project Number: FAP-2017-3164.

5. References

1. N. F. Braga, A. P. da Silva, T. M. Arantes, A. P. Lemes, F. H. Cristovan, *Materials Research Express*, **2018**, **5**. **DOI:**10.1088/2053-1591/aa9f7a
2. M. Oner, B. Ilhan, *Materials Science & Engineering C-Materials for Biological Applications*, **2016**, *65*, 19–26. **DOI:**10.1016/j.msec.2016.04.024
3. G. Keskin, G. Kizil, M. Bechelany, C. Pochat-Bohatier, M. Oner, *Pure and Applied Chemistry*, **2017**, *89*, 1841–1848. **DOI:**10.1515/pac-2017-0401
4. M. Öner, G. Keskin, G. Kızıl, C. Pochat-Bohatier, M. Bechelany, *Polymer Composites*, **2017**.
5. J. L. C. Mayorga, M. J. F. Rovira, L. C. Mas, G. S. Moragas, J. M. L. Cabello, *Journal of Applied Polymer Science*, **2017**, *135*.
6. A. Jaszkiewicz, A. K. Bledzki, A. Meljon, *Journal of Applied Polymer Science*, **2013**, *130*, 3175–3183.
7. Y. Srithep, T. Effingham, J. Peng, R. Sabo, C. Clemons, L. S. Turng, S. Pilla, *Polymer Degradation and Stability*, **2013**, *98*, 1439–1449. **DOI:**10.1016/j.polymdegradstab.2013.05.006
8. A. Dufresne, D. Dupeyre, M. Paillet, *Journal of Applied Polymer Science*, **2003**, *87*, 1302–1315. **DOI:**10.1002/app.11546
9. S. Singh, A. K. Mohanty, M. Misra, *Composites Part a-Applied Science and Manufacturing*, **2010**, *41*, 304–312. **DOI:**10.1016/j.compositesa.2009.10.022
10. A. Javadi, Y. Srithep, S. Pilla, C. C. Clemons, S. Q. Gong, L. S. Turng, *Polymer Engineering and Science*, **2011**, *51*, 1815–1826. **DOI:**10.1002/pen.21972
11. L. Jiang, J. J. Huang, J. Qian, F. Chen, J. W. Zhang, M. P. Wolcott, Y. W. Zhu, *Journal of Polymers and the Environment*, **2008**, *16*, 83–93. **DOI:**10.1007/s10924-008-0086-7
12. S. S. Ahankari, A. K. Mohanty, M. Misra, *Composites Science and Technology*, **2011**, *71*, 653–657. **DOI:**10.1016/j.compscitech.2011.01.007
13. E. Ten, J. Turtle, D. Bahr, L. Jiang, M. Wolcott, *Polymer*, **2010**, *51*, 2652–2660. **DOI:**10.1016/j.polymer.2010.04.007
14. N. F. Magalhaes, K. Dahmouche, G. K. Lopes, C. T. Andrade, *Applied Clay Science*, **2013**, *72*, 1–8. **DOI:**10.1016/j.clay.2012.12.008
15. L. Hassaini, M. Kaci, N. Touati, I. Pillin, A. Kervoelen, S. Bruzaud, *Polymer Testing*, **2017**, *59*, 430–440. **DOI:**10.1016/j.polymertesting.2017.03.004
16. S. Singh, A. K. Mohanty, T. Sugie, Y. Takai, H. Hamada, *Composites Part a-Applied Science and Manufacturing*, **2008**, *39*, 875–886. **DOI:**10.1016/j.compositesa.2008.01.004
17. S. Vidhate, L. Innocentini-Mei, N. A. D'Souza, *Polymer Engineering and Science*, **2012**, *52*, 1367–1374 **DOI:**10.1002/pen.23084
18. S. Kirboga, M. Oner, *Powder Technology*, **2017**, *308*, 442–450. **DOI:**10.1016/j.powtec.2016.11.042
19. T. Thenepalli, A. Y. Jun, C. Han, C. Ramakrishna, J. W. Ahn, *Korean Journal of Chemical Engineering*, **2015**, *32*, 1009–1022. **DOI:**10.1007/s11814-015-0057-3
20. S. Kirboga, M. Oner, *Biointerface Research in Applied Chemistry*, **2016**, *6*, 1320–1326.
21. J. Kalfus J. Jancar, *Polymer Composites*, **2007**, *28*, 365–371. **DOI:**10.1002/pc.20273
22. P. H. T. Vollenberg, D. Heikens, Pol*ymer* **1989,** 30, 1656–1662. **DOI:**10.1016/0032-3861(89)90326-1
23. M. Tanniru, R. D. K. Misra, *Materials Science and Engineering a-Structural Materials Properties Microstructure and Processing*, **2005**, *405*, 178–193. **DOI:**10.1016/j.msea.2005.05.083
24. M. A. Osman, A. Atallah, *Macromolecular Chemistry and Physics*, **2007**, *208*, 87–93. **DOI:**10.1002/macp.200600435
25. Y. Ahn, J. H. Jeon, J. H. Park, T. Thenepalli, J. W. Ahn, C. Han, *Korean Journal of Chemical Engineering*, **2016**, *33*, 3258–3266. **DOI:**10.1007/s11814-016-0159-6
26. R. Thire, L. C. Arruda, L. S. Barreto, *Materials Research-Ibero-American Journal of Materials*, **2011**, *14*, 340–344. **DOI:**10.1590/S1516-14392011005000046
27. A. Neira-Carrillo, P. Vasquez-Quitral, M. Paz Diaz, M. Soledad Fernandez, J. Luis Arias, M. Yazdani-Pedram, *Journal of Solid State Chemistry*, **2012**, *194*, 400–408. **DOI:**10.1016/j.jssc.2012.05.039
28. B. Akin, M. Oner, Y. Bayram, K.D. Demadis, *Crystal Growth & Design* **2008,** 8, 1997–2005. **DOI:**10.1021/cg800092q
29. S. Kerisit, S. C. Parker, J. H. Harding, *Journal of Physical Chemistry B* **2003,** 107, 7676–7682. **DOI:**10.1021/jp034201b
30. Q. Meng, D. Chen, L. Yue, J. Fang, H. Zhao, L. Wang, *Macromolecular Chemistry and Physics*, **2007**, *208*, 474–484.

DOI:10.1002/macp.200600466
31. S. P. Luo, J. Z. Cao, A. G. McDonald, *Acs Sustainable Chemistry & Engineering*, **2016**, *4*, 3465–3476. **DOI:**10.1021/acssuschemeng.6b00495
32. Z. Wu, Z. Zhang, K. Mai, *Journal of Thermoplastic Composite Materials,* **XX**, XX. **DOI:**10.1177/0892705718807955
33. M. Oner, G. Kızıl, G. Keskin, C. Pochat-Bohatier, M. Bechelany, *Nanomaterials*, **2018**, *8*, 940–959. **DOI:**10.3390/nano8110940
34. S. K. Swain, S. Dash, C. Behera, S. K. Kisku, L. Behera, *Carbohydrate Polymers*, **2013**, *95*, 728–732. **DOI:**10.1016/j.carbpol.2013.02.080
35. M. H. Klopffer, B. Flaconneche, *Oil & Gas Science and Technology-Revue D Ifp Energies Nouvelles*, **2001**, *56*, 223–244. **DOI:**10.2516/ogst:2001021
36. M. Avella, M. E. Errico, G. Gentile, *Macromolecular Symposia*, **2006**, *234*, 170–175. **DOI:**10.1002/masy.200650222
37. L. Huang, P.L. Zhu, G. Li, F.R. Zhou, D.Q. Lu, R. Sun, C.P. Wong, *Journal of Materials Science-Materials in Electronics* **2015**, 26, 3564–3572. **DOI:**10.1007/s10854-015-2870-1

Povzetek

Namen te študije je bil z metodo ekstruzije pripraviti poli(3hidroksibutirat-ko-3-hidroksivalerat) biokompozite z dodanimi različnimi odstotki kalcijevega karbonata. Kalcijev karbonat smo sintetizirali v odsotnosti in prisotnosti poli(vinil sulfonske kisline). Polimorfizem in morfologija kalcijevega karbonata sta se spremenila z dodatkom poli(vinil sulfonske kisline). Romboedrski kalcit dobimo v odsotnosti poli(vinil sulfonske kisline). Romboedrski kalcit se je z dodatkom poli(vinil sulfonske kisline) preoblikoval v vaterit. Preučevali smo vpliv vsebnosti polnila na lastnosti poli(3-hidroksibutirat-ko-3-hidroksivalerata) kompozitov. Strukturo in lastnosti biokompozitov poli(3-hidroksibutirat-ko-3-hidroksivalerat)/kalcijev karbonat smo preučevali z naslednjimi metodami: XRD, FTIR, TGA, DSC, SEM, OTR in DMA. Vpliv kalcijevega karbonata na kristalizacijo poli(3-hidroksibutirata-co-3-hidroksivalerata) smo opazili pri meritvah DSC in XRD. Pokazalo se je, da sta na lastnosti biokompozitov vplivala polimorfizem in morfologija kalcijevega karbonata. Dodatek 0,5 % (*w*) romboedrskega kalcita in vaterita je v primerjavi s čistim polimerom povečal stopnjo prenosa kisika (OTR) za 25 % oziroma 12 %. Raziskali smo tudi mehanske lastnosti kompozitov, ki so bile izboljšane ob dodatku kalcita oziroma vaterita.